

Electronic supplementary information

Photo-Induced Charge Kinetic Acceleration in Ultrathin Layered Double Hydroxide Nanosheets Boosts Oxygen Evolution Reaction

Peng Ding,^a Fengting Luo,^a Pengdi Wang,^a Weiwei Xia,^a Xiaoyong Xu,^{*,a,b} Jingguo Hu,^{*,a} and Haibo Zeng^{*,b}

^aCollege of Physics Science and Technology, Yangzhou University, Yangzhou 225002, China

^bInstitute of Optoelectronics and Nanomaterials, College of Materials Science and Engineering Nanjing University of Science and Technology, Nanjing 210094, China

1. Experimental Details

1.1 Preparation of bulk CoFe LDHs: The bulk CoFe LDHs are synthesized by a facile hydrothermal method. First, 0.3 M $\text{Fe}(\text{NO}_3)_3 \cdot 9\text{H}_2\text{O}$ and 0.6 M $\text{Co}(\text{NO}_3)_2 \cdot 6\text{H}_2\text{O}$ (Co/Fe molar ratio of 2:1) were dispersed in deionized water (DIW) and stirred for 30 minutes. Similarly, 1.92 M NaOH and 0.8 M Na_2CO_3 were dispersed in deionized water and stirred for 30 minutes. Subsequently, the above two solutions were mixed with vigorous stirring over 10 minutes, and then the obtained mixture (15 ml) was transferred into a stainless-steel Teflon-lined autoclave (25 ml) for heating for 50 hours in the oven at a constant temperature of 80 °C. When the autoclave cooled naturally to room temperature, the black product was taken out and rinsed repeatedly with DIW/ethanol, and then dried at 60 °C for 12 hours in a vacuum oven.

1.2 Preparation of ultrathin CoFe-LDH NSs: 30 mg of bulk LDHs were loaded into a quartz boat for plasma etching in a plasma reactor (SmartPlasma). The treatments were operated using Ar plasma with pressure of 0.1 mbar and power of 100 W for different reaction times, and the etching time was optimized at 60 min so as to maximize the catalytic activity.

1.3 Electrode preparation: 4 mg of catalyst powder was added to a graduated cylinder, and then 300 μL of ethanol, 30 μL of 5 wt% Nafion solution and 300 μL of DIW were successively injected with sonication for at least 30 min to form a homogeneous ink. The glassy carbon (GC) electrode was polished into a mirror finish and thoroughly cleaned before loading catalysts. Then, 6 μL of the catalyst ink was loaded onto a cleaned GC electrode (2 mm in radius, 0.1256 cm^2 of area), with a constant catalyst loading of 0.3 mg cm^{-2} . The as-fabricated catalyst film supported on GC electrode was dried at room temperature for 12 hours in a vacuum oven.

2. Material Characterizations

SEM was implemented by a Hitachi S-4800II with an accelerating voltage of 15 kV. TEM and HRTEM were taken by a Tecnai F30 equipped with EDX spectroscopy with an acceleration voltage of 200 kV. Powder XRD patterns were recorded on a Shimadzu XRD-7000 diffractometer with Cu $K\alpha$ radiation ($\lambda=1.54 \text{ \AA}$). FT-IR spectroscopy was conducted using a Varian Cary 670 spectrometer. XPS analysis was performed on an ESCALAB250Xi spectrometer using Al $K\alpha$ as an excitation source at 150 W, and the binding energies were calibrated according to the C 1s peak at 284.6 eV. UV-vis diffuse reflectance spectra were recorded on a Cary 5000 spectrophotometer (Varian). PL spectra were obtained by with a FL4600 spectrophotometer (Hitachi) using Xe lamp emission at 400 nm as an excitation source. SPV measurements were performed with monochromatic light source (CHF-

XM-500 W, Global Xenon Lamp Power) through grating monochromator (Omni- λ 3007-MC300) and lock-in amplifier (SR830-DSP) with light chopper (SR540) at chopping frequency of 23 Hz.

3. Performance Measurements

All EC and PEC measurements were performed with a three-electrode system of an electrochemical workstation (CHI-660E Instruments, Shanghai, China) using 1 M KOH (pH=13.8) electrolyte. The GC electrodes loaded with catalysts (0.30 mg) was respectively employed as the working electrodes, the saturated Ag/AgCl electrode was used as the reference electrode, and the graphite rod (Alfa Aesar, 99.9995%) was used as the counter electrode. The LSV curves were recorded at a scan rate of 5.0 mV s⁻¹ to minimize capacitance current and after the multiple scans until to a steady state to better assess the catalytic OER activity. The catalytic activities were measured using the LSV with a scan rate of 5 mV s⁻¹ in 1 M KOH. The Tafel plots were obtained from the linear portion fitting the Tafel equation ($\eta = b \log |j| + a$) to determine the Tafel slopes (b). The simulated 1 sun irradiation (100 mW cm⁻²) was provided by the Xe lamp with an AM 1.5 G filter and calibrated by an irradiatometer. The light response and stability measurements were performed using chronoamperometry and chronopotentiometry techniques, respectively. All the potentials were reported with the *iR* compensation and against the reversible hydrogen electrode (RHE) via following formulas: $E_{\text{corrected}} = E_{\text{measured}} - iR_s$ and $E_{\text{RHE}} = E_{\text{Ag/AgCl}} + 0.059 \times \text{pH} + 0.1976$, where R_s is the EIS-determined series resistance. The EIS was measured with frequencies ranging from 1 MHz to 0.1 Hz at open-circuit voltage with 5.0 mV amplitude. The CV measurements in a small potential range of 1.3-1.4 V with varying scan rates of 2, 4, 6, 8, and 10 mV s⁻¹ were used to estimate C_{dl} values as important indicators of electrochemically active surface areas.

4. Calculation Methods

The mass activity (j_m , A g⁻¹) and site activity (TOF, s⁻¹) were evaluated by normalizations in terms of the catalyst mass and active-site number, respectively. The j_m was calculated by the equation: $j_m = j/m$, where j is the measured current density (mA cm⁻²) and m is the catalyst loading mass (0.3 mg cm⁻²). TOF was calculated by the formula: $\text{TOF} = j/4nF$, where j is the current density (A cm⁻²) in the LSV curve, F is the Farady constant (C mol⁻¹), n is the mole number of active sites per unit area (mol cm⁻²) and the factor 1/4 represents that four electrons are required to form one oxygen molecule. The active-site-density n can be estimated by the equation: $n = C_{\text{dl}} \times \Delta V / 2F$, where C_{dl} and ΔV are the double-layer capacitance (C_{dl} , F cm⁻²) and the voltage window (V) for CV measurements, and their product ($C_{\text{dl}} \times \Delta V$) is the voltammetric charge density (Q , C cm⁻²), and the factor 1/2 is due to the charge-discharge cycles for CV scans.

5. Additional Characterizations and Measurements

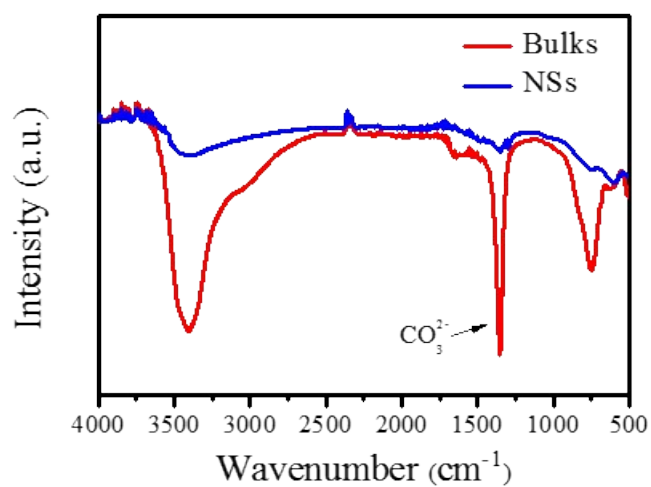


Figure S1. FT-IR spectra of CoFe-LDH bulks and NSs.

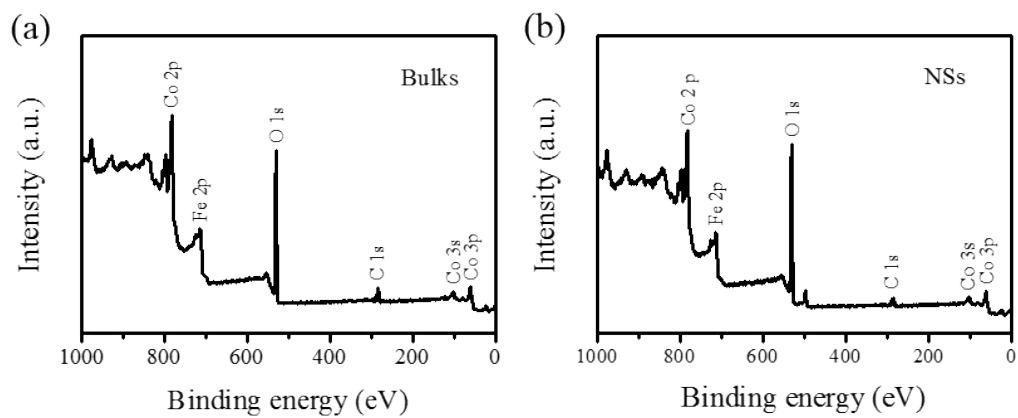


Figure S2. XPS survey spectra of CoFe-LDH (a) bulks and (b) NSs.

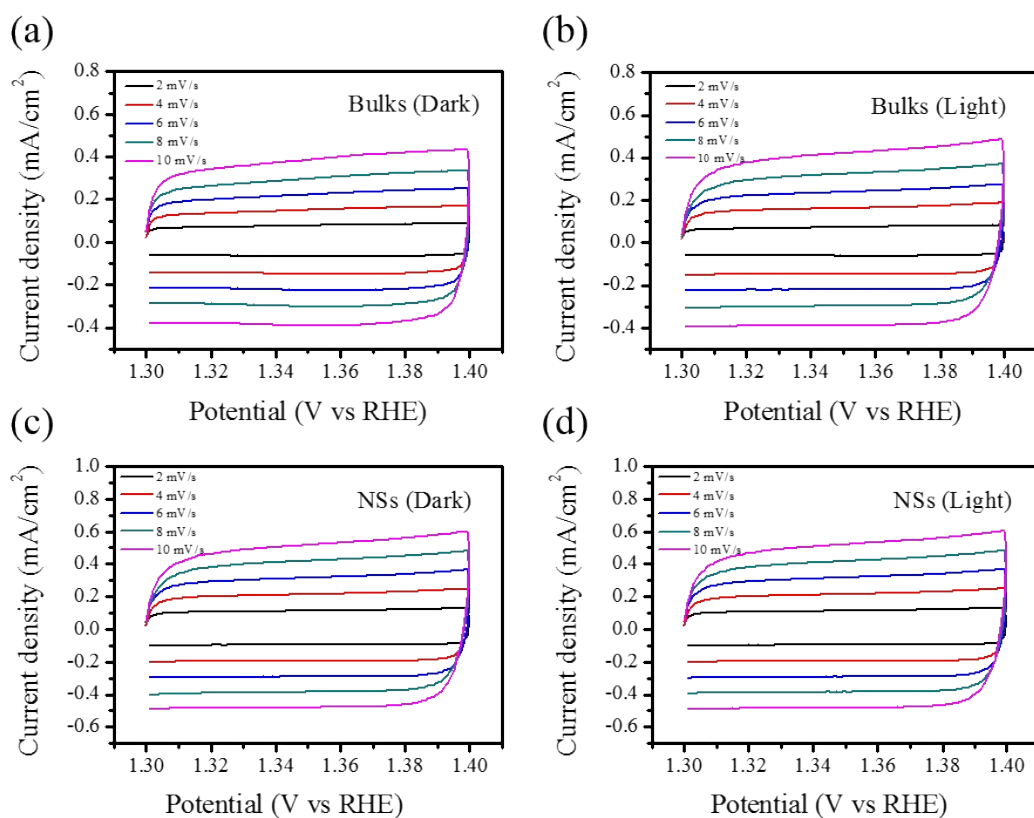


Figure S3. CV curves of (a, b) CoFe-LDH bulks and (c, d) NSs in dark and light fields at different potential scanning rates.

The scan rates are 2, 4, 6, 8 and 10 mV s^{-1} . The selected potential range where no faradic current was observed is 1.3 to 1.4 V vs. RHE. The halves of the positive and negative current density differences at the center of the scanning potential ranges were plotted versus the voltage scan rate to determine their EASAs.

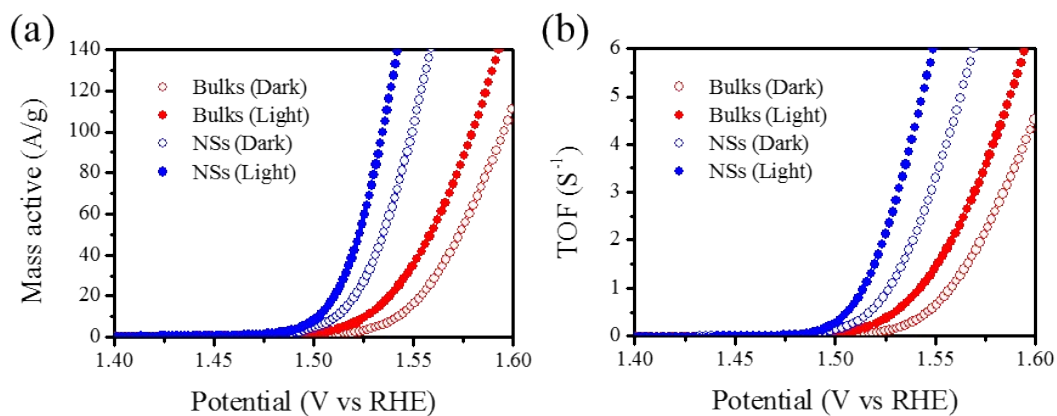


Figure S4. Mass activities and TOFs of OER for CoFe-LDH (a) bulks and (b) NSs in dark and light fields.

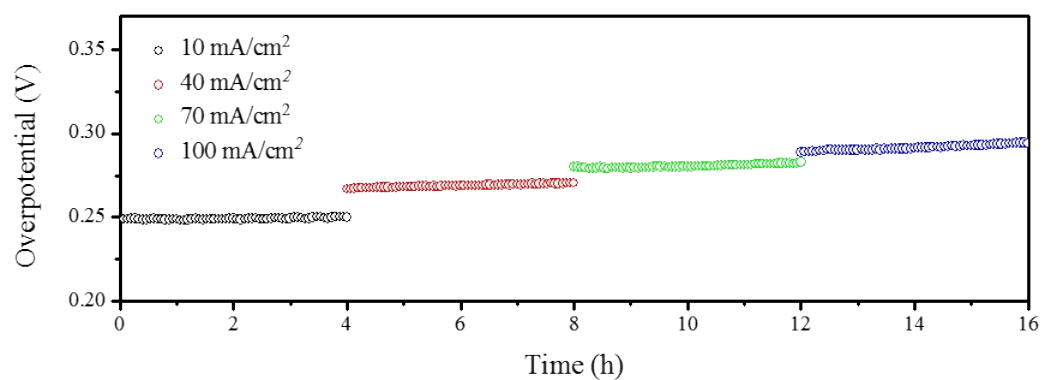


Figure S5. Chronopotentiometry curve for CoFe-LDH NSs supported on Ni foam with varying current densities from 10 to 100 mA cm⁻² under 1 sun irradiation.

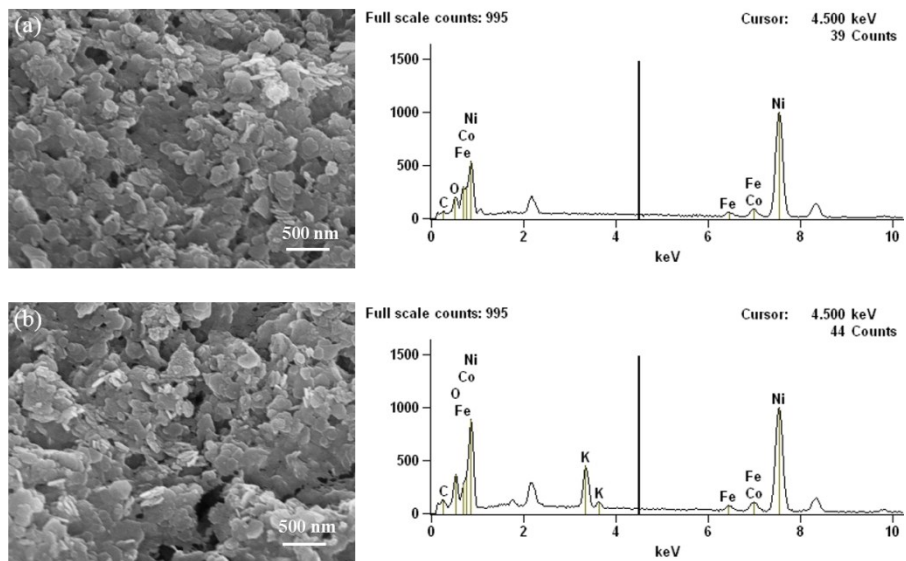


Figure S6. SEM images with EDS analyses of CoFe-LDH NSs supported Ni foam (a) before and (b) after stability testing. K ions come from the electrolyte (KOH).

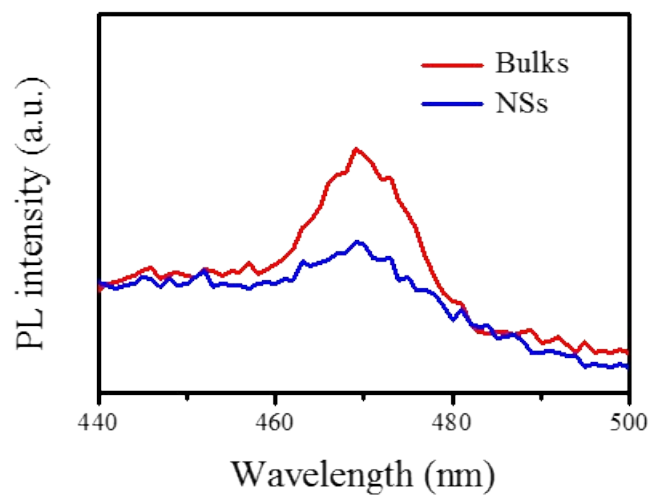


Figure S7. Room-temperature PL spectra of CoFe-LDH bulks and NSs.

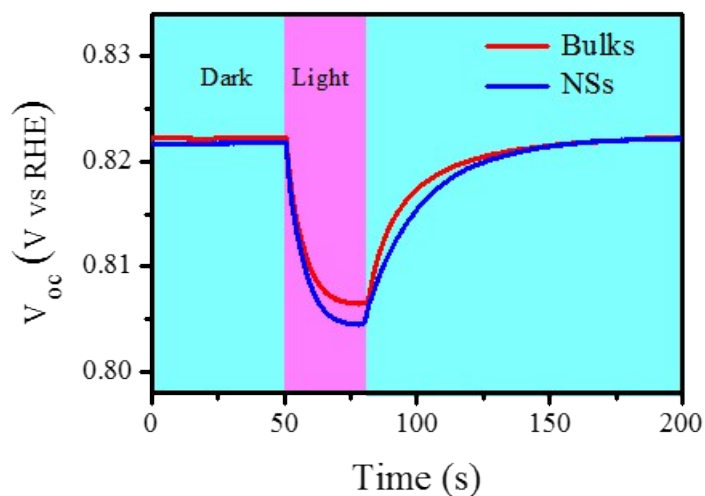


Figure S8. Time dependent V_{oc} for CoFe-LDH bulks and NSs upon ON/OFF switched light irradiation.

When the light irradiation at open circuit is terminated, the charge recombination kinetics on the electrode surface is relevant to the photovoltage decay rate. The electron lifetimes (τ) at different potentials can be determined from the V_{oc} decay using the following equation:

$$\tau = -\frac{k_B T}{e} \left(\frac{dV_{oc}}{dt} \right)^{-1}$$

where k_B is Boltzmann's constant, T is the temperature, and e is the elementary charge. The comparison of V_{oc} decay upon irradiation termination reveals the longer survivability of photogenerated charge in the CoFe-LDH NSs.

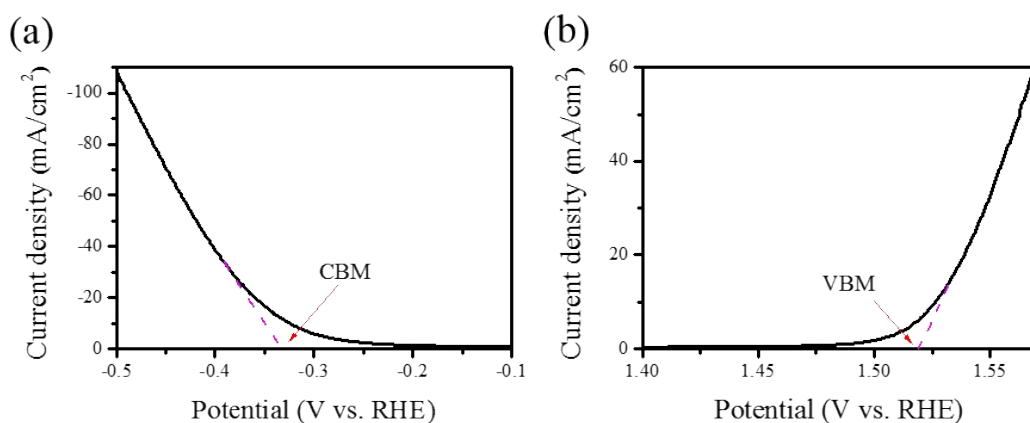


Figure S9. Cathodic and anodic scans at 5 mV s^{-1} to determine the CBM and VBM for the CoFe-LDH NSs.

In the LSV, applying potentials above the CBM to form an accumulation layer and below the VBM to form an inversion layer, can bring about the abrupt emergence of cathodic and anodic currents, respectively. The energy levels of CBM and VBM are estimated to be around -0.32 and $1.3 \text{ V}_{\text{RHE}}$, respectively.

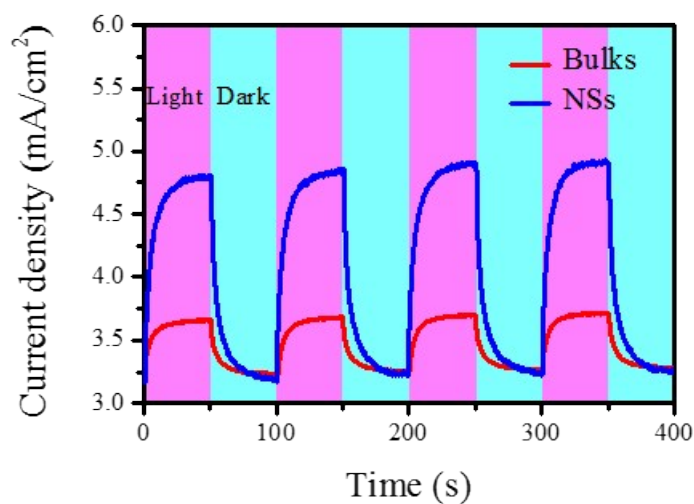


Figure S10. Photocurrent response spectra of CoFe-LDH bulks and NSs at certain overpotential of 270 mV upon ON/OFF switched 1 sun irradiation.

Table S1. Comparison of various OER catalysts recently reported in the literatures.

Catalyst	Overpotential@ 10 mA/cm ² (mV)	Tafel slope	Mass active (A/g) @1.53 V	Substrate	Reference
NiCo-LDH NSs	299	45	22.5	CFP	1
NiFe-PBA	283	54	98	GC	2
Fe-CoOOH	330	37	15	GP	3
Co ₄ Fe(OH) _x	295	52	50	GC	4
FeCo(O) NSs	308	36.8	26.39	GC	5
Ni ₃ FeN NPs	280	46	NM	NF	6
CoN NWs	290	70	11.3	NF	7
CoFe ₂ O ₄ NSs	275	42.1	48.6	GC	8
CoFe-LDH NSs	280	55	NM	CFP	9
CoFe-LDH NSs	295 (dark)	34	38.5	GC	This Work
	281 (light)	28	98.6		

Note: GC-glass carbon; GP-graphene; NF-nickel foam; CFP-carbon fiber paper; NM-no mention.

REFERENCES

- [1] Liu, Y. Q.; Zhang, M.; Hu, D.; Li, R. Q.; Hu, K.; Yan, K. Ar Plasma-Exfoliated Ultrathin NiCo-Layered Double Hydroxide Nanosheets for Enhanced Oxygen Evolution. *ACS Appl. Energy Mater.* 2019, 2, 1162–1168.
- [2] Yu, Z. Y.; Duan, Y.; Liu, J. D.; Chen, Y.; Liu, X. K.; Liu, W.; Ma, T.; Li, Y.; Zheng, X. S.; Yao, T.; Gao, M. R.; Zhu, J. F.; Ye, B. J.; Yu, S. H. Unconventional CN Vacancies Suppress Ironleaching in Prussian Blue Analogue Pre-catalyst for Boosted Oxygen Evolution Catalysis. *Nat. Commun.* 2019, 10, 2799.
- [3] Han, X. T.; Yu, C.; Zhou, S.; Zhao, C. T.; Huang, H. W.; Yang, J.; Liu, Z. B.; Zhao, J. J.; Qiu, J. S. Ultrasensitive Iron-Triggered Nanosized Fe-CoOOH Integrated with Graphene for Highly Efficient Oxygen Evolution. *Adv. Energy Mater.* 2017, 7, 1602148.
- [4] Jin, H. Y.; Mao, S. J.; Zhan, G. P.; Xu, F.; Bao, X. B.; Wang, Y. Fe Incorporated α -Co(OH)₂ Nanosheet with Remarkably Improved Activity towards Oxygen Evolution Reaction. *J. Mater. Chem. A*, 2017, 5, 1078–1084.
- [5] Zhuang, L. Z.; Ge, L.; Yang, Y. S.; Li, M.; Jia, Y.; Yao, X. D.; Zhu, Z. H. Ultrathin in Iron-Cobalt Oxide Nanosheets with Abundant Oxygen Vacancies for the Oxygen Evolution Reaction. *Adv. Mater.* 2017, 29, 1606793.
- [6] Jia, X. D.; Zhao, Y. F.; Chen, G. B.; Shang, L.; Shi, R.; Kang, X. F.; Waterhouse, G. I. N.; Wu, L.; Tung, C.; Zhang, T. R. Ni₃FeN Nanoparticles Derived from Ultrathin NiFe-Layered Double Hydroxide Nanosheets: An Efficient Overall Water Splitting Electrocatalyst. *Adv. Energy Mater.* 2016, 6, 1502585.
- [7] Zhang, Y. Q.; Ouyang, B.; Xu, J.; Jia, G. C.; Chen, S.; Rawat, R. S.; Fan, H. J. Rapid Synthesis of Cobalt Nitride Nanowires: Highly Efficient and Low-Cost Catalysts for Oxygen Evolution. *Angew. Chem. Int. Ed.* 2016, 55, 1–6.

- [8] Fang, H. Y.; Huang, T. Z.; Liang, D.; Qiu, M.; Sun, Y.; Yao, S.; Yu, J. M.; Dinesh, M. M.; Guo, Z. Q.; Xia, Y.; Mao, S. Prussian Blue Analog-Derived 2D Ultrathin CoFe_2O_4 Nanosheets as High-activity Electrocatalysts for Oxygen Evolution Reaction in Alkaline and Neutral Mediums. *J. Mater. Chem. A* 2019, 7, 7328–7332.
- [9] Sahanaz, P.; Dhirendra, K. C.; Anima, G.; Sayan, B. Attuning The Electronic Properties of Two-Dimensional Co-Fe-O for Accelerating Water Electrolysis and Photolysis. *ACS Appl. Mater. Interfaces* 2019, 11, 30682–30693.